National Aeronautics and Space Administration

Orbital Debris Quarterly News

Volume 23, Issue 3
August 2019

Inside...

A publication of the NASA Orbital Debris Program Office (ODPO)

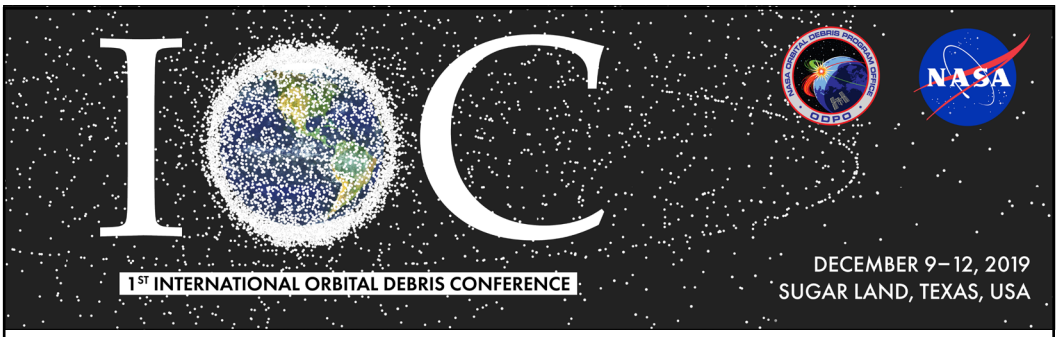

The First International Orbital Debris Conference (IOC) is scheduled for December 9–12, 2019 at the Sugar Land Marriott Town Square in Sugar Land (greater Houston area), Texas.

Visit the conference website for registration and logistics information.

https://www.hou.usra.edu/meetings/orbitaldebris2019/

The program and abstracts are available on this website. Register by November 10 for the best conference rates and by November 21 for hotel reservations at the group rate.

ODQN readers are referred to the conference website for the roster of keynote speakers.

Two Breakup Events Reported

The Indian spacecraft Microsat-R (International Designator 2019-006A, U.S. Strategic Command [USSTRATCOM] Space Surveillance Network [SSN] catalog number 43947), launched on 24 January 2019, was intentionally destroyed in a test of a ground-based, direct-ascent Anti-Satellite (ASAT) weapon system at 0640 GMT on 27 March 2019. At the time of breakup the 740 kg spacecraft was in an approximately 294 x 265 km altitude, 96.63° orbit. A total of 101 debris have entered the public satellite catalog (through object 2019-006DF), of which 49 fragments remain on-orbit as of 15 July 2019. However, over 400 fragments were initially tracked by SSN sensors and cataloging is complicated by the low altitude of the event and the concomitant rapid orbital decay. A Gabbard plot of this debris cloud is presented in the figure on page 2.

A Centaur V Single-Engine Centaur (SEC) rocket variant (International Designator 2018-079B, SSN number 43652) fragmented in early April 2019. At the time of the event the stage was in an approximately 35,092 x 8526 km altitude, 12.2° orbit. This Centaur V upper stage is associated with the launch of the USA 288, or Advanced Extremely High Frequency 4 (AEHF 4), spacecraft from the (U.S.) Air Force Eastern Test Range on 17 October 2018. The cause of the event is unknown. No debris have entered the catalog at this time, but the ODQN will provide updates should they become publicly available. ♦

continued on page 2

Breakup Events

continued from page 1

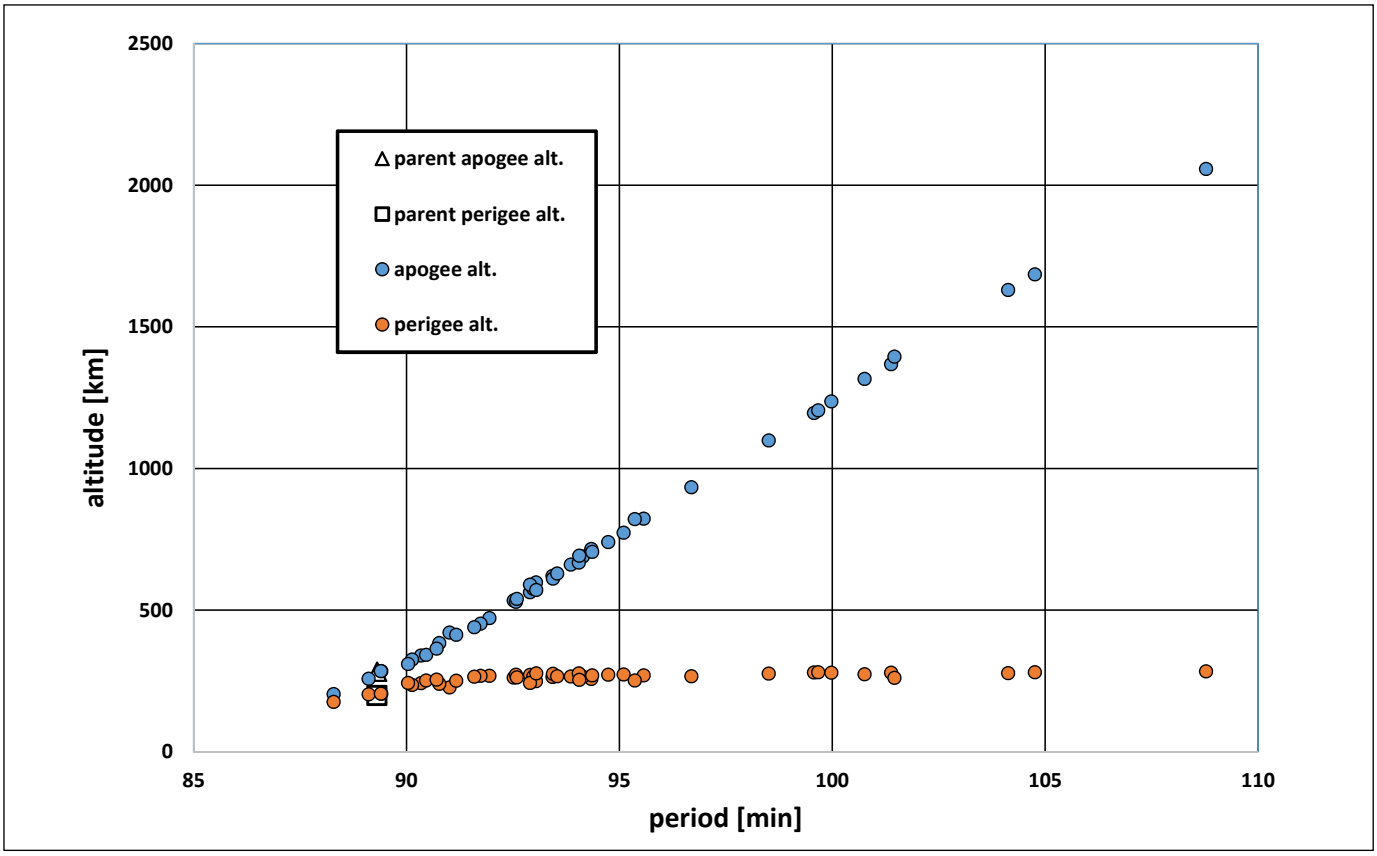

The Microsat-R fragments Gabbard plot. Epoch is approximately 5 June 2019. Maximum change in period is on the order of 19 minutes. Maximum change in inclination is on the order of 2°.

NASA Technical Standard *Process for Limiting Orbital Debris* Revision Ratified

This revision of the NASA Technical Standard (NS) 8719.14 is mandated by the formal NASA acceptance of the revised governing policy document NPR 8715.6 (to revision B) in February 2017 (*Procedural Requirements for Limiting Orbital Debris and Evaluating the Meteoroid and Orbital Debris Environments*). Revision NS 8719.14B addresses three key areas:

1. Changes bring NS 8719.14 revision B into full compliance with the current U.S. Government (USG) Orbital Debris Mitigation Standard Practices (ODMSP). With revision B of the standard, NASA now disallows long-term disposal options that cross through the semi-synchronous MEO band occupied by the Global Positioning System. The revised standard also brings requirement 4.3-2 into alignment with the USG ODMSP for sizes of allowed debris, and takes steps to limit the quantity and orbital lifetime of swarms of satellites smaller than 1U CubeSats.

2. The revised NPR 8715.6 simplifies the documentation content and delivery schedule and the required signatures at different stages of certain document deliveries. Such changes have been incorporated into the revised NS 8719.14B, and the required forms have been simplified.

3. The revision cleans up confusing or obsolete wording (especially related to active flight of the shuttle).The revision has included the support and contributions of spacecraft developers across all NASA centers since the policy itself was in formation. In the final draft over 85% of the comments from these developers have been accepted in whole or in part, and concurrence has been obtained from the authors of all suggestions that were not incorporated.

The Orbital Debris Program Office has prepared the supporting Debris Assessment Software version 3.0 (DAS 3.0) for public release. DAS 3.0 incorporates the updated requirements and reporting details to support compliance with the updated standard. The software will be released in the near future.

NS 8719.14 revision B is expected to have a retirement date of 25 April 2024 in keeping with the required periodic update of NPR 8715.6. It is possible that with the release of updated USG ODMSP in the near future, there may be impetus to update both the policy and standard earlier than currently specified. ♦

PROJECT REVIEW

Testing and Modeling the Demisability of Fiber-Reinforced Plastics

B. GREENE, C. SANCHEZ, AND C. OSTROM

A key component of orbital debris mitigation is the disposal of spacecraft at end of mission. The best post-mission plan from an orbital debris mitigation standpoint removes the spacecraft from orbit entirely within a reasonable period after the end of the spacecraft's useful life, and atmospheric reentry, whether targeted or through gradual orbital decay, is often an inexpensive and effective means to do this. However, accurate modeling of the thermal demise of the spacecraft is required for assessing the casualty risk to people on the ground due to randomly falling debris from spacecraft disposed of in such a manner.

As previously reported (ODQN, vol. 22, issue 3, September 2018, p. 3), the NASA Orbital Debris Program Office (ODPO), in association with the Johnson Space Center's Structural Engineering Division and the University of Texas (UT) at Austin, tested the demisability of several fiber-reinforced polymer (FRP) materials that have become common in modern spacecraft, but whose reentry behavior is not currently well-modeled. For classical aerospace materials like aluminum and titanium, the primary mode of demise is melting of the material. However, polymer-based materials like FRPs tend to char and chemically decompose through the process of pyrolysis rather than melting, invalidating certain assumptions of this classical demise model.

The Phase I test results have prompted development of a new material model for the Object Reentry Survival Analysis Tool (ORSAT) that more accurately models the behavior of carbon fiber-reinforced polymer (CFRP) during reentry.

Experimental Facility and Setup

The materials were tested at the Inductively Coupled Plasma torch facility at UT Austin. The facility uses a 50 kW induction coil to superheat up to 1.5 g/s of test gas to approximately 6000 K or a specific enthalpy of between 15 and 40 MJ/kg [1]. To insert probes and test articles into the plasma stream, the facility includes a motorized dual-arm water-cooled insertion mechanism.

A total of 95 material samples were investigated for effects of fiber material, fiber weave structure, honeycomb core, and oxygen content of the plasma stream on the demisability of composite materials. Table 1 lists the material samples used and the shape and fiber weave, if applicable. Each material was exposed to both an argon plasma with a heat flux of 30 W/cm^2 and an air plasma with a heat flux of 60 - 80 W/cm^2 at both the midpoint and the end of the tube.

Table 1. Test Sample Descriptions and Quantities

Material	Shape	Weave	Quantity
Aluminum	Rod	N/A	7
Fiberglass	Rod	Unidirectional (axial)	9
Kevlar	Tube	Bi-directional cross-weave	10
Carbon Fiber	Tube	Spiral wound	17
Carbon Fiber	Tube	Bi-directional cross-weave	19
Carbon Fiber	Tube	Planar, unwoven	18
Carbon Fiber	Rod	Unidirectional (axial)	10
G10	Plate	N/A	3
CFRP-Al honeycomb	Plate	Bi-directional cross-weave	2

Small objects, such as spacecraft fragments entering the atmosphere from a ~120 km circular decay orbit, typically experience a peak heat flux between 10 and 80 W/cm^2 and a dynamic pressure of between 0.1 and 10 kPa, depending on the shape and ballistic coefficient of the object.

The tests focused on CFRP since spacecraft fragments made from these materials have been shown to survive to the ground, contrary to demise predictions [2]. However, glass fiber-reinforced polymer (GFRP) and Kevlar-reinforced polymer were also studied.

Test Results

Of the three classes of FRP tested, Kevlar demonstrated the highest demisability. The samples demised within 35 seconds of exposure to the completely non-oxidizing plasma environment, quickly pyrolyzing both the polymer matrix and the Kevlar fibers, as shown in Fig. 1.

The fiberglass rods displayed very different behavior from that of the Kevlar samples. When exposed to a non-oxidizing plasma, the polymer matrix pyrolyzed and was quickly removed from the material. However, the glass fibers remained and slowly melted until the section exposed to the plasma could no longer support the weight at the end of the rod, and the sample was considered to have demised. The result of this test is shown in Fig. 2 and indicates that in the absence of oxidation, the primary mode of demise is melting of the glass fibers, which is consistent with the assumptions made in ORSAT.

CFRP, on the other hand, displayed a high resistance to thermal demise in this series of tests, with samples exposed to oxidizing plasma taking up to 4 minutes to fully demise and samples exposed to non-oxidizing plasma never reaching the demise condition within the allotted test period.

Different CFRP samples were exposed for various amounts of time to measure the mass loss rate over the course of the demise process. The results for the non-oxidizing argon plasma condition are shown in Fig. 3. The mass loss rate is initially high and asymptotically approaches zero as the polymer matrix is pyrolyzed. Because graphite sublimation will not occur below a surface temperature of 3000 K, without an oxidizer to ablate the carbon fibers they remain indefinitely.

In an oxidizing atmosphere, the mass loss shows a different trend, a bilinear curve, shown in Fig. 4, as the matrix is first removed through pyrolysis, and then the slower process of graphite

continued on page 4

Figure 1. Kevlar sample exposed until demise.

Figure 2. Sample of axially oriented GFRP inserted in argon plasma for 80 seconds (considered demised).

Testing Demisability

continued from page 3

oxidation removes the fibers. In this environment, the samples completely demised in approximately 250 seconds. This is much greater than the typical duration of peak plasma heating during reentry, with oxygen flux many times that of actual entry, indicating that all of these samples would have survived the reentry process.

ORSAT CFRP Material Model

The results of the UT Austin plasma torch experiments showed much greater survivability of CFRP materials than previously assumed and prompted the development of a new material model to serve as a transitional "two-material" model. It is recommended for immediate use in ORSAT 6.2 to bring spacecraft demise predictions more in line with experimental data until an ablation model can be developed. For users of the Debris Assessment Software (DAS), the two-material model is not applicable due to the reduced feature set of DAS's reentry risk assessment module as compared to ORSAT. Instead, the upcoming DAS 3.0 release conservatively assumes that all CFRP components will survive reentry intact.

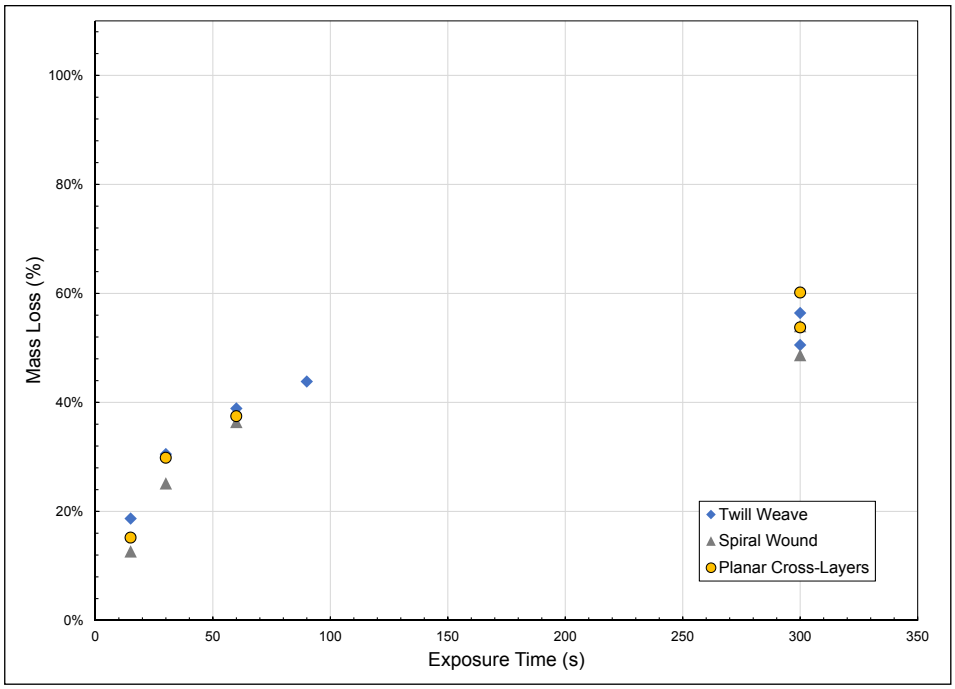

Figure 3. Mass loss of CFRP tubes in argon plasma.

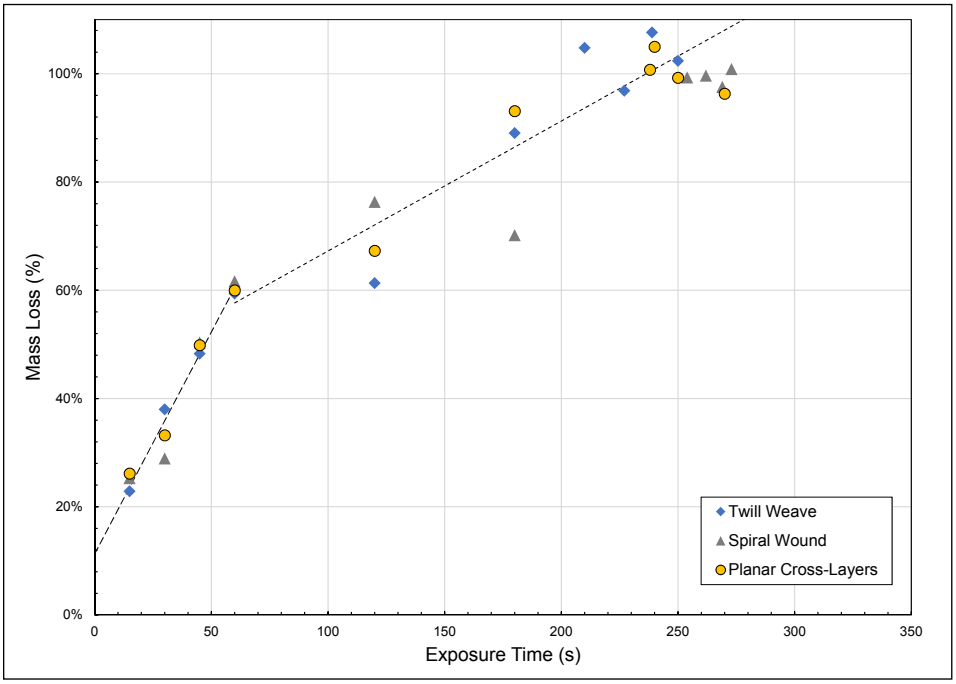

Figure 4. Mass loss of CFRP tubes in air plasma as percentage of mass directly exposed to plasma.

The underlying assumption of this new model is that all the epoxy in a CFRP or GFRP component will pyrolyze and be removed from the composite. The removal of the epoxy from the composite is also assumed to have a minimal effect on the thickness of the composite – currently modeled to cause a reduction of 5% of the object's wall thickness.

The CFRP or GFRP component is modeled as two distinct homogeneous phases: a thin outer layer of pseudo-epoxy and a thick inner layer of pseudo-carbon, with the thermal conductivity and heat capacity tailored to match that of the bulk material. Due to the design in ORSAT's user-defined materials, the specific heat capacity and thermal conductivity of the bulk material are described by a linear regression of the temperature-dependent values for Graphite Epoxy 1 (Eqs. 1 and 2). Values for emissivity, melting point temperature, heat of fusion, and oxide heat of formation are taken as constants, and can be seen for both phases in Table 2.

$$C_{p,CFRP}(T) = 10.726 + 2.7539 * T \quad (1)$$

$$k_{CFRP}(T) = 0.4224 + 3.7669 * 10^{-4} * T \quad (2)$$

Table 2. Constant Material Property Values for Epoxy and Carbon Components of CFRP Material Model

Property	Epoxy	Carbon
Emissivity	0.9	0.9
Melting Point (K)	700	3915
Latent Heat of Fusion (J/kg)	2326	9999999
Oxide Heat of Formation (J/kg-O_2)	12305781	0

The volume of each phase is calculated assuming a thickness for the pseudo-epoxy layer of

continued on page 5

Testing Demisability

continued from page 4

5% of the total thickness of the material (Eq. 3), and then the density of each phase is set such that the total mass of the material and mass fraction of polymer and matrix is preserved (Eqs. 4-8). The calculated density of each phase is then used to weight the thermal conductivity such that the temperature response of the two phases is identical to that of the original Graphite Epoxy 1 model (Eqs. 9 and 10).

$$V_C = V(shape, L, W, H, 0.95t) \quad (3)$$

$$V_E = V_{CFRP} - V_C \quad (4)$$

$$M_E = M_{CFRP} * EF \quad (5)$$

$$\therefore M_{CFRP} - M_E \quad (6)$$

$$\rho_C = \frac{M_C}{V_C} \quad (7)$$

$$\rho_E = \frac{M_E}{V_E} \quad (8)$$

$$C_{p,C}(T) = \frac{\rho_{CFRP}}{\rho_C} C_{p,CFRP}(T) \quad (9)$$

$$C_{p,E}(T) = \frac{\rho_{CFRP}}{\rho_E} C_{p,CFRP}(T) \quad (10)$$

References

1. Greene, B.R., *et al*. "Characterization of a 50 kW Inductively Coupled Plasma Torch for Testing of Ablative Thermal Protection Materials," The 55th Aerospace Sciences Meeting, Grapevine, TX, (2017).

2. Lips, T., *et al*. "About the Demisability of Propellant Tanks During Atmospheric Re-Entry from LEO," The 8th IAASS Conference, Melbourne, FL, USA, (2016). ♦

An Extended Parametric Study of the Effects of Large Constellations on the Future Debris Environment

D. GATES, A. VAVRIN, A. MANIS, J.-C. LIOU, AND M. MATNEY

Over the past few years, several commercial companies—notably OneWeb and SpaceX—have proposed telecommunications constellations consisting of hundreds to thousands of 100- to 300-kg-class spacecraft in low Earth orbit (LEO). If deployed, such large constellations (LCs) could contribute to the existing orbital debris problem and create a challenge for the safe operations of future missions. The NASA Orbital Debris Program Office (ODPO) recently completed a parametric study on LCs to quantify the potential negative debris-generation effects of LCs on the LEO environment (see ODQN, vol. 22, issue 3, September 2018, pp. 4-7).

The planned constellations are expected to be designed to comply with the existing orbital debris mitigation measures for removing spacecraft from orbit via atmospheric reentry within 25 years of retirement, and for limiting the probability of explosion to less than 0.001. In many cases, the planned reentry of these constellation spacecraft is 5 years after retirement. However, past experiences such as the Iridium satellite constellation suggest that to minimize the risk to the space environment at their specific operational altitudes, constellation operators will need to make refinements to future constellation spacecraft in order to comply with standard practices.

Therefore, with thousands of spacecraft anticipated to be added to the LEO environment in the near future, it is of paramount importance to understand and assess the risk that these constellations pose to the usability and safety of the LEO space environment. In this review, we explore extended scenarios of the NASA ODPO LC study (ODQN 22-3) by assuming that the post-mission disposal rates and explosion probabilities of LC spacecraft vary with time, representing improvements to spacecraft systems and operations.

All scenarios are modeled using the NASA ODPO LEO-to-GEO ENvironment Debris (LEGEND) numerical simulation model [1]. The background future launch traffic cycle is assumed to be a repeat of the launches over 8 years of the recent historical period. The historical period covers launches through the end of 2015, and the future projection begins in 2016. For all scenarios, the background post mission disposal (PMD) of non-constellation spacecraft and rocket bodies is fixed at 90%. Background spacecraft and rocket bodies are allowed to explode according to accidental explosion probabilities derived from historical explosion events. Additionally, collisions between objects greater than 10 cm are assessed statistically.

In addition to this background population, three LCs are modeled to operate from 1000 km to 1325 km altitudes with different inclinations and orbital planes. The three constellations comprise a total of 8300 spacecraft. The masses of individual spacecraft are 150 kg for constellations A and B, and 300 kg for constellation C. Each spacecraft is deployed at 500 km altitude, raises its orbit to mission altitude, operates for 5 years, then conducts PMD operations to lower its orbit such that it will naturally decay in 5 years. Then the spacecraft is replaced by a new one.

Furthermore, it is assumed that conjunction assessments and collision avoidance maneuvers are conducted for LC spacecraft that have successful deployment, operations, and PMD through final reentry. In addition, because the planned mission lifetime for the proposed constellations is 5 years, we assume the constellation is replenished every 5 years for 20 years.

The effectiveness of increasing PMD rates and decreasing explosion probabilities over time for LC spacecraft is determined based upon the increase in effective number of objects greater than 10 cm in LEO at the end of 200 years. The effective number is defined as the fractional time, per orbital period, that an object remains in LEO. For each of these scenarios the projected debris population is taken as the average of 100 Monte Carlo (MC) simulations of the LEGEND model.

Post-mission Disposal of Constellations

The first assessment covers the effect of allowing the successful PMD rate of the constellation spacecraft to vary over the 20-year constellation lifetime for each replenishment cycle and/or spacecraft generation. For all scenarios in this set, the accidental explosion probability of LC spacecraft is consistent with spacecraft in the background population. A control scenario is used for comparison, in which all background and LC spacecraft maintain a PMD rate of 90%. Five additional scenarios are considered with

continued on page 6

Effects of Large Constellations

continued from page 5

PMD rates that vary with the LC replenishment cycles. Table 1 shows the PMD rates applied to LC spacecraft in each replenishment cycle, *i.e.*, every 5 years after the initial 5-year set of LC spacecraft, for each constellation scenario.

Figure 1 shows the increase in the effective number of total LEO objects for each scenario in Table 1, as well as the control scenario, over the 200-year projection, whereas Table 1 gives the percent difference in effective number of objects, relative to the control scenario, after the 200-year projection for time-varying LC PMD rates.

From Fig. 1 and Table 1, comparing the control scenario (PMD 90%) to Scenario 1a reveals that improvements in PMD per constellation as small as 1% per replenishment cycle yield 11% fewer objects in orbit at the end of 200 years, as compared to the control scenario. This suggests that incremental PMD improvement via experience operating the constellations and/or improved spacecraft design can have a non-negligible effect on the future debris environment.

Additionally, comparing Scenarios 2a and 3a with the control demonstrates that if operators have problems initially with the logistics of controlling hundreds or sometimes thousands of spacecraft, it will have a significant effect on the future space environment. For Scenario 2a, which incorporates a PMD improvement from the 1st generation at 80% to the 2nd generation at 85% and then to the 3rd generation at 90%, the effective number of objects after 200 years is approximately 9% higher than the control case. Scenario 3a, in which the initial PMD rate is significantly lower at 60% but increases to 90% in the first two replenishment cycles, doubles this relative increase with approximately 18% more objects in orbit after 200 years, relative to the control scenario.

Explosion Rate of Constellations

For the second set of LC scenarios considered here, the background PMD is fixed at 90% for non-constellation objects, as before, and the PMD rate of constellation spacecraft also is fixed at 90%. In addition, because the planned mission lifetime for the proposed constellations is 5 years, we assume the constellation is replenished every 5 years for 20 years, exactly as before. The control scenario used here exhibits an accidental explosion probability for LC spacecraft of 1/1000 over a 5-year mission lifetime. Four additional scenarios are considered that exhibit decreasing probabilities of explosion for LC spacecraft over each replenishment cycle, representative of improved reliability of spacecraft with each cycle. The time-varying explosion rates are shown in Table 2.

Figure 2 shows the increase in the effective number of objects for each scenario in Table 2, as well as the control scenario, over the 200-year projection. Table 2 presents the percent difference in effective number of objects, relative to the control scenario, after the 200-year projection for time-varying LC probabilities of explosion. Consider Scenarios 1b and 4b to represent companies targeting explosion rates as the mode of improvement for future constellation spacecraft by decreasing the LC explosion probabilities from 1/1000 to 1/5000 or 1/16000, respectively, over the 20-year constellation. For these scenarios, we see a reduction of 2.5% and 5%, respectively, in the total effective number of objects in the environment after 200 years, relative to the control scenario. Thus, it is reasonable to conclude that designing to control explosion probability further than 1/1000 for later constellations has a small return on investment and supports previous results (ODQN 22-3) that an explosion probability of 1/1000 is sufficient for protecting the future orbital debris environment.

In Scenario 2b, the probability of explosion for the earliest set of LC spacecraft is 1/250, improving to 1/500 after 5 years, and then 1/1000 for the remainder of the 20-year constellation. In this scenario, the environment has 7.1% more effective number of objects at the end of 200 years than the control. Scenario 3b, in parallel with the PMD Scenario 4b, represents the case in which the first set of LC spacecraft has a probability of explosion 10 times higher than the ideal 1/1000 explosion probability, but the spacecraft design is quickly improved by targeting the accidental on-orbit explosion failure mode and the subsequent cohorts meet the target explosion rate. In this scenario, the environment has 13.6% more objects at the end of the simulation relative to the control scenario of 1/1000 probability.

Unlike the PMD Scenarios 4a and 5a, constellations that significantly fail to meet the explosion rate criteria initially but then achieve the target explosion rate at the first replenishment cycle (Scenario 3b), have a markedly worse effect on the future debris environment, as seen by the

continued on page 7

Table 1. PMD Rates Applied to Each LC Spacecraft at Each Replenishment Cycle, i.e., Every 5 Years from the Start of the Constellation and Resulting Simulation Outcomes

Scenario	1st Gen.	2nd Gen.	3rd Gen.	4th Gen.	5th Gen.	% Difference after 200 years
1a	90%	91%	92%	93%	94%	-11%
2a	80%	85%	90%	90%	90%	+8.7%
3a	60%	80%	90%	90%	90%	+17.7%
4a	60%	90%	90%	90%	90%	+2%
5a	60%	95%	95%	95%	95%	-54%

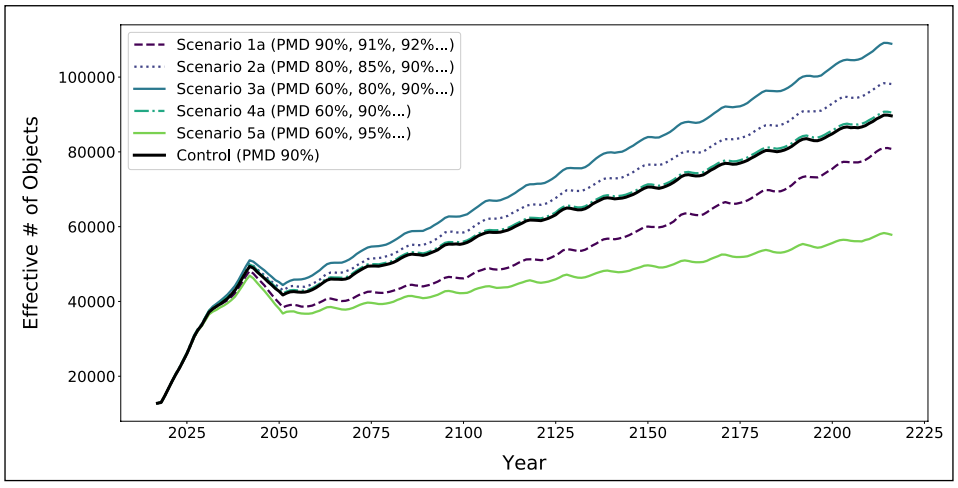

Figure 1. Effective number of objects projected to be in orbit after 200 years with varying PMD success rates over each replenishment cycle. The bulge represents the constellations deploying and the subsequent fall-off represents the end of the constellations lifetime, i.e., there are no more additional constellations being added to the environment.

Effects of Large Constellations

continued from page 6

increase of almost 14% over the control scenario when compared to only 2% in the case of PMD Scenario 4a. In fact, achieving a factor of 10 reduction in the accidental explosion probability of LC spacecraft at the first replenishment cycle (Scenario 3b) has a similar relative effect on the environment after 200 years as delaying improvement of a low PMD rate to the target rate until the second replenishment cycle (Scenario 3a).

Conclusion

We have shown that improving PMD rates and probabilities of explosion over the 20-year lifetime of a large constellation of spacecraft can have a significant effect on the future debris environment. With nearly 11% fewer objects in orbit at the end of 200 years as a result of increasing the PMD rate by as little as 1% per constellation replenishment, as compared to a constant PMD rate of 90% for the entire 20-year constellation lifetime, it is in the best interest of constellation operators to continuously improve the PMD rate of their spacecraft over time. In addition, delaying improvements to PMD rates for the first two constellations could have a dramatic negative impact on the future debris environment with 9% to 18% more objects in orbit after 200 years. This supports the NASA ODPO conclusion that maximizing PMD for the constellations from first launch is of paramount importance.

In terms of maintaining a low accidental probability of explosion, it was demonstrated that failing to meet a threshold of explosion probability of 1/1000 for the first constellation cohort has a noticeable negative effect on the projected debris environment, yielding nearly 14% more objects in orbit after 200 years if the first set of spacecraft deployed has a high probability of explosion of 1/100. Therefore, constellation operators should design spacecraft to ensure an accidental probability of explosion of 1/1000 or better from the initial constellation deployment in order to protect the future space environment.

Reference

1. Liou, J.-C., *et al*. "LEGEND – A Three-Dimensional LEO-to-GEO Debris Evolutionary Model," Adv. Space Res., vol. 34, pp. 981-986 (2005). ♦

Table 2. Probabilities of Explosion Applied to Each LC Spacecraft at Each Replenishment Cycle, i.e., Every 5 Years from the Start of the Constellation and Resulting Simulation Outcomes

Scenario	1st Gen.	2nd Gen.	3rd Gen.	4th Gen.	5th Gen.	% Difference after 200 years
1b	1/1000	1/2000	1/3000	1/4000	1/5000	-2.5%
2b	1/250	1/500	1/1000	1/1000	1/1000	+7.1%
3b	1/100	1/1000	1/1000	1/1000	1/1000	+13.6%
4b	1/1000	1/2000	1/4000	1/8000	1/16000	-5.0%

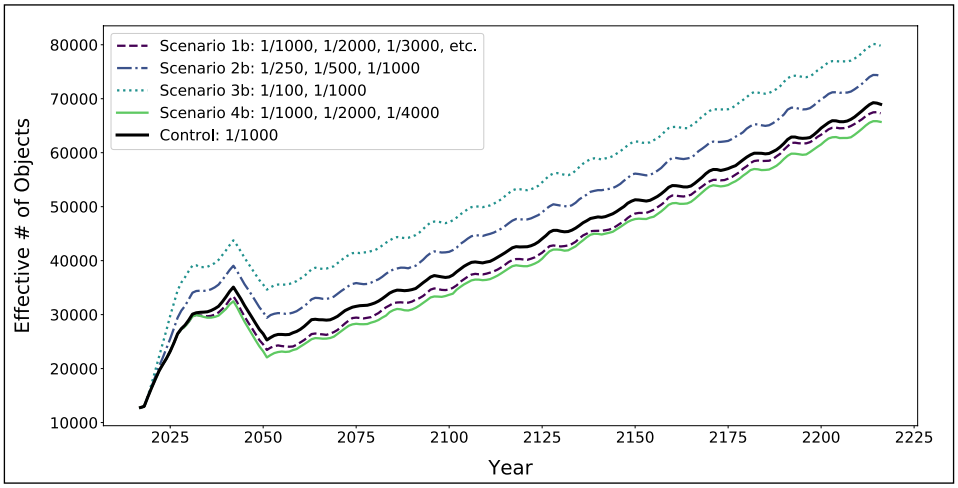

Figure 2. Effective number of objects projected to be in orbit after 200 years with varying explosion rates over each replenishment cycle. The bulge represents the constellations deploying and the subsequent fall-off represents the end of the constellations lifetime, i.e., there are no additional constellations being added to the environment.

MEETING REPORTS

The 15th Hypervelocity Impact Symposium, 15-19 April 2019, Destin, Florida, USA

The 15th Hypervelocity Impact Symposium (HVIS) was held in Destin, Florida, on 15-19 April 2019. The HVIS is a biennial events organized by the Hypervelocity Impact Society and serves as the principal forum for presenting the physics of high- and hypervelocity impact and related technical areas.

This year's symposium was coordinated by the Department of Mechanical Engineering at the University of Alabama at Birmingham and attracted more than 228 attendees from government, industry, and academic organizations.

The Hypervelocity Impact Symposium consisted of 11 topical oral and poster sessions. These covered high-velocity launchers and diagnostics, spacecraft meteoroid/debris shielding and failure analyses, material response to hypervelocity impacts, fracture and fragmentation, high-velocity penetration mechanics, armor/anti-armor and non-linear analytical/numerical methodologies for structural dynamics. A total of 72 oral and 25 poster papers were presented representing the community's latest efforts to better characterize hypervelocity impact phenomenology and solar system impacts.

The NASA Hypervelocity Impact Team's Josh Miller was co-chair for the Technical Session 8 on Analytical and Numerical Methodologies 1. Papers specific to impact observations of returned surfaces and impact observations of operational assets were presented, along with papers describing the structural response of spaceborne assets. Abstracts submitted from HVIT are located on pp. 8-10 of this issue. The Orbital Debris Program Office's entry was published in ODQN Vol. 23, Issue 1 & 2, p. 10. The society adjourned its meeting and will reconvene in September of 2021 in the Washington DC area. ♦

MEETING REPORTS - *continued*

continued from page 7

10th International Association for the Advancement of Space Safety (IAASS) Conference, 15-17 May 2019, El Segundo – Los Angeles, California, USA

The 10th IAASS Conference was held 15-17 May 2019 in El Segundo, California at the headquarters of the Aerospace Corporation, with nearly 200 attending members from the global space safety community.

The conference was comprised of 28 technical sessions and 4 plenary sessions, covering topics from launch safety, human factors, space traffic control, space sustainability, space debris, design-for-safety, laws, regulation and standards, risk management, and reentry safety.

The conference opened with keynotes from George Gafka, the Chief Safety Officer for NASA Johnson Space Center's Office of Safety and Mission Assurance (SMA); Takumi Ujino, the Associate Director General and Senior Chief Officer of SMA at JAXA; and James Wade, the Vice President of Mission Assurance at Raytheon. The NASA ODPO participated in the "Reentry Safety – I" and "Reentry Safety – II" with three presentations, titled "Effect of Latitude Bias in Entry Angle on Ground Casualty Risk from Naturally Decaying Space Objects," "Seasonal- and Beta-Angle-Dependent Latitude Bias Variations in Natural Decays," and "Demisability of Various Reinforced Polymer Components of Reentering Orbital Debris: Phase I Test Results," providing a full overview of the ODPO's improvements in statistical modeling of atmospheric reentry, as well as the first phase of testing of carbon-fiber- and glass-fiber-reinforced plastics (see ODQN, vol. 22, issue 3, September 2018, pg. 3, "Spacecraft Material Ablation Testing at UT Austin"). ♦

32nd International Symposium on Space Technology and Science, 15-21 June 2019, Fukui, Japan

The 32nd International Symposium on Space Technology and Science (ISTS) took place in Fukui, Japan, on 15-21 June 2019. Visit https://www.ists.or.jp/index.html to see the full program.

This year's ISTS was a joint conference with the 9th Nano-Satellite Symposium (NSAT), with a conference theme of "Fly like a Phoenix to Space." The symposium also celebrated its 60th year, having first met in 1959. For the third consecutive year, the 2019 ISTS comprised over 1000 participants.

The Opening Ceremony highlighted talks from Hiroshi Sasaki, Director, Japan Aerospace Exploration Agency (JAXA) Space Exploration Center (JSEC); Naoki Sato, Director, Space Exploration System Technology Unit, JSEC; Tomohiro Usui, Professor, Department of Solar System Sciences, Institute of Space and Astronautical Science (ISAS); and Tatsuaki Hashimoto, SLS Launched CubeSats Project Team Leader, ISAS. The Deputy Director General of ISAS, Masaki Fujimoto, served as the moderator for the panel discussion "International Space Exploration," which featured the recent development and plans including mission scenarios to the Moon and Mars. Dr. Sandra Magnus, former NASA astronaut, provided a well-received keynote speech on "Navigating to the Stars: The Challenges and Opportunities for the Space Industry in the Coming Decades."

A total of 24 papers were presented during the space debris sessions on 19 June and 20 June. Papers focused on observation, collision risk assessment, in-situ measurements, cataloging, modeling, protection, and active debris removal. The ISTS "Space Debris (Cataloging, In-situ Measurement, and Modeling)" sessions were chaired by Rongyu Sun from the Chinese Academy of Sciences and Kumi Nitta from JAXA. Two papers representing NASA ODPO were presented in this session: Drew Vavrin (Jacobs JETS/NASA ODPO) presented "Summary of the NASA Large Constellations Parametric Study" and Drake Gates (Jacobs JETS/NASA ODPO) presented "An Extended Parametric Study of the Effects of Large Constellations on the Future Debris Environment."

While all papers addressed topics of interest to the general ODQN readership, three notable papers were Shengxian Yu "A Dynamical Criterion for Catalogue Correlation of Space Debris," Masahiro Furumoto "Improvement in an Estimation Method of the Debris Environment Utilizing In-situ Measurements," and Rongyu Sun "Optical Survey and Catalogue Space Object in High Earth Orbital Region." ♦

ABSTRACTS FROM THE NASA HYPER-VELOCITY IMPACT TECHNOLOGY TEAM

2019 Hypervelocity Impact Symposium (HVIS 2019), 14-19 April 2019, Destin, Florida, USA

Prediction of Micrometeoroid Damage to Lunar Construction Materials using Numerical Modeling of Hypervelocity Impact Events

M. ALLENDE, J. MILLER, A. DAVIS, E. CHRISTIANSEN, M. LEPECH, AND D. LOFTUS

The use of Lunar regolith for the creation of construction materials to build habitats and other Lunar base infrastructure is an example of in situ resource utilization, an important strategy to minimize a NASA mission's launch mass by leveraging materials found at an exploration destination. One class of solidified regolith, Biopolymer-bound Soil Composites (BSC), consists of regolith mixed with a small amount of biopolymer binding agent (10% w/w). This paper characterizes BSC's micrometeoroid impact performance using experimental and numerical methods. Micrometeoroids are a notable hazard of the lunar environment and pose a challenging design consideration. A total of 17 hypervelocity impact experiments were conducted on BSC targets at NASA's White Sands Testing Facility. Numerical simulations of the hypervelocity impact experiments were carried out using

continued on page 9

Prediction of Micrometeoroid Damage - continued

continued from page 8

CTH, a shock physics code developed by Sandia National Laboratories. Comparisons between the experimental craters and the simulation results indicate that there is good agreement between crater dimensions of the hypervelocity impact experiments and the CTH model. The CTH model developed in this paper provides (1) a damage prediction tool that allows for the necessary extrapolation of micrometeoroid impact velocities beyond what is experimentally achievable and into the velocity regime that is relevant for micrometeoroids and (2) a material design tool that is capable of varying material parameters computationally, ultimately allowing for the engineering and optimization of BSC's performance under impact loading. ♦

Hypervelocity Impact Performance of 3D Printed Aluminum Panels

B. DAVIS, R. HAGEN, R. MCCANDLESS, E. CHRISTIANSEN, AND D. LEAR

With the continued development of additive manufacturing methods, control over the shape of ligaments, cell regularity, and macroscopic shape can all be easily tuned. This capability allows for tailoring of component architecture and promotes potential mass savings in a space vehicle structure. Additionally, it allows the flexibility of combining structural elements such as MMOD protection and vehicle stiffness for launch loads for an overall mass reduction. At NASA JSC this technology is being explored in many different ways with the goal being a multifunctional structural component. For this study, four different types of aluminum panels have been 3D printed for testing, three being of a body centric cubic (BCC) lattice structure core and one being kelvin cell structure core. All samples have a 0.127 cm (0.05") nominally thick aluminum face sheet printed on the front and back side of each panel, with all core materials having a 5.08 cm (2.0") nominal. These tests will evaluate the performance of 3D printed aluminum panels under hypervelocity impact (HVI) conditions.

The hypervelocity impact tests are being conducted at the JSC White Sands Test Facility (WSTF) Remote Hypervelocity Test Laboratory (RHTL), located in Las Cruces, New Mexico. All tests will be conducted with a 3.4 mm Al 2017-T4 sphere at 6.8 km/s impacting at 0° to surface normal (*i.e.*, impacting with no obliquity). Each sample will be trapped between two metal frames, with gasket material residing between the sample and frame, which will be the shipping and testing configuration for all tests. There will be an Al 2017-T4 witness plate staged 5.08 cm (2.0") from each sample to capture signature of debris, if the rear face sheet of the sample were to perforate from the HVI test event. ♦

Consequences of Micrometeoroid/Orbital Debris Penetrations on the International Space Station

H. EVANS, J. HYDE , E. CHRISTIANSEN, AND D. LEAR

Risk from micrometeoroid and orbital debris (MMOD) impacts on space vehicles is often quantified in terms of the probability of no penetration (PNP). However, for large spacecraft, especially those with multiple compartments, a penetration may have a number of possible outcomes. The extent of the damage (diameter of hole, crack length, or penetration depth), the location of the damage relative to critical equipment or crew, crew response, and even the time of day of the penetration are among the many factors that can affect the outcome. For the International Space Station (ISS), a Monte-Carlo style software code called Manned Spacecraft Crew Survivability (MSCSurv) is used to predict the probability of several outcomes of an MMOD penetration—broadly classified as loss of crew (LOC), crew evacuation (EVAC), loss of escape vehicle (LEV), and nominal end of mission (NEOM). By generating large numbers of MMOD impacts (typically in the hundreds of billions) and tracking the consequences, MSCSurv allows for the inclusion of a large number of parameters and models as well as enabling the consideration of uncertainties in these models and parameters. MSCSurv builds upon the results from NASA's Bumper software (which provides the probability of penetration and critical input data to MSCSurv) to allow analysts to estimate the probability of LOC, EVAC, LEV, and NEOM. This paper provides an overview of the methodology used by NASA to quantify LOC, EVAC, LEV, and NEOM with particular emphasis on describing in broad terms how MSCSurv works and its capabilities and most significant models. ♦

Extravehicular Activity Micrometeoroid and Orbital Debris Risk Assessment Methodology

K. HOFFMAN, J. HYDE, E. CHRISTIANSEN, AND D. LEAR

A well-known hazard associated with exposure to the space environment is the risk of vehicle failure due to an impact from a micrometeoroid and orbital debris (MMOD) particle.

Among the vehicles of importance to NASA is the extravehicular mobility unit (EMU) "spacesuit" used while performing a U.S. extravehicular activity (EVA). An EMU impact is of great concern as a large leak could prevent an astronaut from safely reaching the airlock in time, resulting in a loss of life. For this reason, a risk assessment is provided to the EVA office at the Johnson Space Center (JSC) prior to certification of readiness for each U.S. EVA.

To assess the risk of failure, a detailed finite element model (FEM) of the EMU has been created, which has regions for the various shielding configurations. Each shielding configuration is based on the layers and materials over the innermost bladder layer that maintains the acceptable atmospheric environment for the astronaut. Ballistic limit equations (BLE) for each shielding configuration have been determined from hypervelocity impact testing of samples of the EMU layup.

Timelines of each EVA provide the major worksite locations on the International Space Station (ISS) for each of the EVA tasks, and EVA training runs in the Neutral Buoyancy Lab (NBL) determine the appropriate body orientation at each worksite. From this information, the FEM is produced for the specific EVA, which includes multiple EMU FEMs (placed at each worksite location) on a simplified ISS FEM to take into account the effect of shadowing (protection) offered by the ISS structure.

The EVA FEM, along with the MMOD environment files (which predict an impacting particle flux based on inputs for orbital parameters, spacecraft attitude, and analysis date), are input into the Bumper-3 code to determine a probability of failure for a nominal EVA from the sporadic environment. To address events outside of the background environment, environment factors from the Orbital Debris Program Office at JSC and the Meteoroid Program Office at Marshall

continued on page 10

Extravehicular Activity MMOD Assessment Methodology - continued

continued from page 9

Spaceflight Center (MSFC) are used to account for recent orbital debris breakup events and meteor shower activity in the probability of failure. The culmination of the analysis is an EVA risk, like that shown in Figure 1 for a recent, typical EVA. As can be seen in the risk contour, the EVA risk assessment indicates that the gloves, arms, and legs are the riskiest regions of the EMU with respect to failures as a result of MMOD. ♦

Numerical Modeling of Impacts of Twisted-pair Data Cables

J. MILLER

Data wire cable runs are a significant presence on the exterior of the International Space Station (ISS), and continued ISS mission support requires detailed assessment of cables due to micrometeoroid and orbit debris (MMOD) impact. These data wire cables are twisted-pair cables consisting of two 22-gauge stranded conductors inside a tight fitting, braided-copper shield and jacket having a nominal outer diameter of 3.76 mm. The ISS engineering community has identified two loss-of-function mechanisms for these cables: open circuits due to severed conductors within the cable, and short-circuits due to contact between conductors or grounded components. Previous work has documented a total of 97 impact experiments that have been performed into these cables to develop an empirical, statistical model for the failure of these cables in reliability studies; however, the experimental work leaves open the internal behaviors that contribute to the probabilistic findings. To address this shortcoming, numerical impact simulations have been performed to expand the understanding of the acquired dataset. ♦

Simulation Study of Non-spherical, Graphite-Epoxy Projectiles

J. MILLER

The DebriSat hypervelocity impact experiment, performed at the Arnold Engineering Development Center, is intended to update the catastrophic break-up models for modern satellites. To this end, the DebriSat was built with many modern materials including structural panels of carbon-fiber, reinforced-polymer (CFRP). Subsequent to the experiment, fragments of the DebriSat have been extracted from porous, catcher panels used to gather the debris from the impact event. Thus far, one of the key observations from the collected fragments is that CFRP represents a large fraction of the fragments and that these fragments tend to be thin, flake-like structures or long, needle-like structures; whereas, debris with nearly equal dimensions is less prevalent. As current ballistic limit models are all developed based upon spherical impacting particles, the experiment has pointed to a missing component in the current approach that must be considered. To begin to understand the implications of this observation, simulations have been performed using cylindrical structures at a representative orbital speed into an externally insulated, double-wall shield that is representative of shielding on the current International Space Station crew transport vehicle, the Soyuz. These simulations have been performed for normal impacts to the surface with three different impact angles-of-attack to capture the effect on the shield performance. This paper documents the simulated shield and the models developed to study the effect of fragments and derives the critical characteristics of CFRP impacting particles for the selected shield. This work gives a deployable form of a critical, non-spherical projectile ballistic limit equation for evaluating non-spherical space debris for orbital debris environment modeling. ♦

ABSTRACTS FROM THE NASA ORBITAL DEBRIS PROGRAM OFFICE

10th International Association for the Advancement of Space Safety (IAASS) Conference, 15-17 May 2019, El Segundo – Los Angeles, California, USA

Seasonal- and Beta-Angle-Dependent Latitude Bias Variations in Natural Decays

J. BACON

Prior work has demonstrated pronounced statistical clustering of natural decays of medium-to-high-inclination orbital objects. The 122-km threshold signalling the final dive to aerothermal breakup tends to cluster approximately 30 degrees in Argument of Latitude (ArgLat) ahead of nodal crossings, and the overall ballistic number of the spacecraft then governs how far downrange the debris will fall. This clustering effect is caused by the physical bulge in the Earth and the overlying atmosphere that cyclically modifies effective altitude (and therefore atmospheric density) in more dramatic fashion than the trajectory's spiralling decay itself. All prior work has averaged seasonal and beta angle effects over all possibilities to support long-term characterization of such clustering of final entries. However, the un-averaged data has shown a wide dispersion that leads to the question of the factors that drive such variation. The current study characterizes seasonal and beta angle effects as predictable influences on this latitude biasing effect. Such influences significantly affect the statistical risks of tactical decay scenarios relative to the average. Such effects can be important considerations in any scenario where small orbital adjustments are contemplated to optimize the timing and location of final entry trajectories. ♦

IAASS Conference - continued

continued from page 10

Demisability of Various Reinforced Polymer Components of Reentering Orbital Debris: Phase I Test Results

B. GREENE AND C. SANCHEZ

A series of tests were conducted by NASA's Orbital Debris Program Office to evaluate the accuracy of material demise models for reentering orbital debris used in NASA's Object Reentry Survival Analysis Tool (ORSAT) and Debris Assessment Software (DAS). Observations of surviving reentry debris on the ground indicated that significantly more glass fiber-reinforced plastic (GFRP) and carbon fiber-reinforced plastic (CFRP) components survive reentry than current models predict.

Phase I tests were conducted at the University of Texas-Austin in the Inductively Coupled Plasma torch Facility. In Phase I tests, a total of 95 samples of materials were tested, including: aluminum, CFRP, Kevlar FRP, GFRP, and G10 (high-pressure fiberglass laminate, composite material). The majority of the samples were cylindrical in shape; with two flat plate samples of G10 and two flat plate samples CFRP/Al honeycomb laminate. The materials were exposed to conditions approximating the reentry environment, using both atmospheric pressure oxidative and non-oxidative environments. Typical heat flux conditions for reentering spacecraft are 30-50 W/cm^2, but due to restrictions of the facility, the cold wall heat flux tested for each gas mixture was 65-85 W/cm^2 and 30-40 W/cm^2, respectively. The cylindrical CFRP samples were exposed to the plasma at both the end and the midpoint in order to investigate the difference in demisability between parts with exposed edges, like panels, and parts with no edges, like carbon-overwrapped pressure vessels (COPVs).

Samples were tested for incremental mass loss and time to complete demise. In a non-oxidative environment, no composite materials demised within the 5-minute test time. In the oxidative elevated heat flux environment, CFRP samples demised in between 210 s and 270 s. For the first 100 s of insertion time, most of the mass loss is due to pyrolysis of resin, creating an approximately bi-linear mass loss rate curve with time. In a non-oxidative environment, carbon filaments were observed to unravel from some of the CFRP end-burned samples; however, this effect did not seem to significantly affect the overall time to thermal demise for the samples. These results indicate that both GFRP and CFRP components survive reentry with significantly more remaining mass than current models predict.

Phase II tests are planned and will focus on obtaining more accurate heat conduction and mass loss information in order to improve the material ablation models for these materials. Mechanical strength tests are also planned for the samples that have already been tested in order to determine the likelihood of mechanical breakup of weakened material due to aerodynamic forces. ♦ (for full article, see pg. 3)

Effect of Latitude Bias in Entry Angle on Ground Casualty Risk from Naturally Decaying Space Objects

C. OSTROM

An improvement to the long-term estimation of ground casualties from naturally decaying space objects is the refinement to the distribution of entry angle at the entry interface as a function of latitude. Previous analyses were based on an assumed "small angle," typically ~0.1 degrees. This study expands on work by Bacon and Matney that indicated there is significant latitude bias in the location of reentries, compared to prior assumptions of equal temporal probability.

A new model has been developed, which describes the distribution of entry angle as a function of orbital inclination and argument of latitude. This model has been used to generate inputs for ODPO's certified reentry survivability software, ORSAT. These new results are compared with the prior standard model to assess the magnitude of the effects on reentry casualty risk. ♦

32nd International Symposium on Space Technology and Science (ISTS), 15-21 June 2019, Fukui, Japan

A Parametric Study of the Effects of Large Constellations on the Future Debris Environment

D. GATES, A. VAVRIN, A. MANIS, J.-C. LIOU, AND M. MATNEY

In recent years, several commercial companies have proposed telecommunications constellations consisting of hundreds to thousands of 100-to-300-kg class spacecraft in low Earth orbit (LEO). If deployed, such large constellations (LCs) could dramatically contribute to the existing orbital debris problem. The NASA Orbital Debris Program Office (ODPO) recently completed a parametric study on LCs to quantify the potential negative debris-generation effects from LCs to the LEO environment.

For the parametric study presented in this paper, we extend the previous study to further analyse the debris-generation potential of LCs based on their post-mission disposal (PMD) rate and probability of explosion. The ODPO's Large Constellation Study assumed that spacecraft at mission altitude conduct post-mission disposal maneuvers (PMD) to lower their orbits to follow the 25-year decay rule at some fixed rate, (*e.g.*, 90%), with a fixed probability of explosion, (*e.g.*, 1/1000), for the lifetime of the constellation. For this parametric study, the PMD rate is allowed to increase over time with each replenishment, *e.g.*, 90%, 93%, 95%, *etc.*, for the initial constellation, first replenishment, and second replenishment, respectively, and the explosion probability is allowed to subsequently decrease to 1/10000. This represents improvements that may be made to increase a LC spacecraft's ability to successfully complete PMD maneuvers and mitigate the risk of explosion over time. In addition, the original study assumed the number of constellation objects was fixed over the constellation lifetime, *i.e.*, the same number of constellation objects was assumed to be replenished after the operational lifetime of the originals expired. For this study, the number of objects per constellation is allowed to vary; this represents a deviation from the planned number of constellation objects as companies adjust replenishment schedules based on successes and failures in the original constellation and allows for the possibility that new companies will deploy constellations. For each of these scenarios and subsequent cohorts we generated the projected debris population as the average of 100 Monte Carlo (MC) simulations of the ODPO's LEO-to-GEO Environment Debris (LEGEND) numerical simulation model. ♦ (for full article, see pg. 5)

ISTS Conference - continued

continued from page 11

Summary of the NASA Large Constellations Parametric Study

A. VAVRIN, A. MANIS, D. GATES, J.-C. LIOU, AND M. MATNEY

In recent years, several commercial companies have proposed telecommunications constellations consisting of hundreds to thousands of 100-to-300-kg class spacecraft in low Earth orbit (LEO, the region below 2000-km altitude). If deployed, such large constellations (LCs) will dramatically change the landscape of satellite operations in LEO. From the large number of spacecraft and large amount of mass involved, it is clear that the deployment, operations, and frequent de-orbit and replenishment of the proposed LCs could significantly contribute to the existing orbital debris problem.

To better understand the nature of the problem, the NASA Orbital Debris Program Office (ODPO) recently completed a parametric study on LCs. The objective was to quantify the potential negative debris-generation effects from LCs to the LEO environment and provide recommendations for mitigation measures. The tool used for the LC study was the ODPO's LEO-to-GEO Environment Debris (LEGEND) numerical simulation model, which has been used for various mitigation and remediation studies in the past. For the LC study, more than 300 scenarios based on different user-specified assumptions and parameters were defined. Selected results from key scenarios are summarized in this paper. ♦

ODQN Vol. 23, Issue 1&2 Errata

Following the publication of "*Analysis of the Stable Laplace Plane for the Observation of Geosynchronous Debris*" (ODQN, Vol. 23, Issue 1&2, pp. 4-6) the ODQN editor was contacted by a reader noting a discrepancy between results presented therein and the reader's independent analysis. In particular, the discrepancy concerned the results presented in the article's Fig. 4, which presents the Laplace plane's inclination as a function of area-to-mass ratio. A detailed examination of differences indicate the discrepancy derives from a choice in the interpolation scheme used to fit the data and in particular, the interpolator's cost function; this function over-penalized a positive concavity. The function was modified and subsequent analysis revealed that a fourth order fit was more appropriate to capture the correct behavior of the data. The revised fit coefficients are: $c_0(x) = 7.33466646$, $c_1(x) = 2.83026815e-02$, $c_2(x) = 1.15366673e-02$, $c_3(x) = -2.07045257e-04$, and $c_4(x) = 1.06303514e-06$.

The reader is reminded that this curve is not a valid solution for values above 40 m^2/kg; it was meant as an *ad hoc* means to formulate a potential observation campaign. As always, physical observations will inform ODPO models and the results in this article will not compromise those models.

Readers should also note that the article's Reference 4 was published in 2014.

The ODQN staff and authors wish to thank Dr. Fabien Gachet for bringing his concerns and comments to our, and the readership's, attention. ♦

Orbital Debris Analyst, Second in an Occasional Series

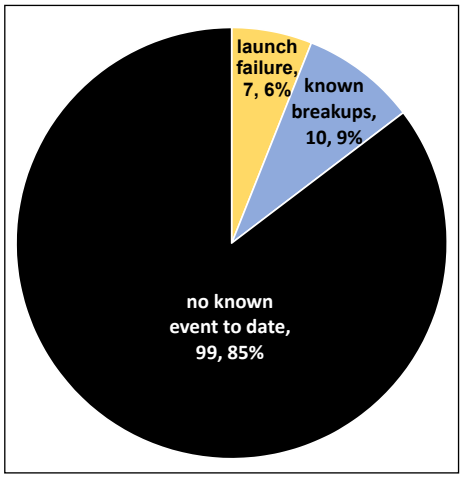

The flight outcomes, to date, for pre-mitigation Delta and Delta II second stage rocket bodies. Annotations include category, number, and percentage of the 116 flights of a common-bulkhead second stage in that category. Note that, though unlikely, the number of known breakups could increase among the limited number of pre-Delta 155 stages still on-orbit due either to new events or identification and cataloging of historical events, ala Delta 52 (ODQN, Vol. 21, Issue 3, p. 1).

This feature acknowledges the fifth anniversary of the last known fragmentation event associated with the Delta and Delta II second stages, now retired, by examining the effectiveness of stage passivation for orbital debris mitigation. Fragmenting on 28 April 2014, the ARGOS/Ørsted/SUNSAT rocket body (International Designator 1999-008D, U.S. Strategic Command Space Surveillance Network catalog number 25637) produced a minor cloud, with seven new debris entering the public satellite catalog and none remaining on orbit as of 5 June 2019.

While no single cause fits all the historical Delta second stage fragmentation data, the highest-likelihood attribution is the mixing of hypergolic propellants through a breach in the common bulkhead separating the fuel and oxidizer tanks. With this attribution, now-standard mitigation practices were introduced with the launch of Delta 155 in August 1981. These practices consist of disabling the range safety ordnance and burning and/or venting remaining propellants and pressurants to depletion. Prior to this mitigation-driven operational procedure, Delta flights 34-154 inclusive experienced 10 known breakups. Afterwards, Delta flights 155-381 inclusive experienced only two known breakups. However, noting the number of debris cataloged in the pre- and post-mitigation operational regimes, pre-mitigation flights produced 1786 debris while post-mitigation flights produced only 34. Further, examining debris remaining on-orbit as of 4 July 2018, the information cut-off date of the 15th edition of the NASA "History of On-orbit Satellite Fragmentations," 1073 pre-mitigation flight debris remain, versus only 2 for post-mitigation Delta fragmentation events. The significantly different nature of the post-mitigation events argues strongly that, indeed, the operational procedures for stage passivation introduced with Delta 155 resulted in a complete success in addressing the highest likelihood fragmentation scenario.

This record for a completed launch program of Delta and Delta II second stages reinforces the effectiveness of standard mitigation practices in promoting the long-term viability of the low Earth orbit environment. ♦

DAS 2.1 NOTICE

Attention DAS 2.1 Users: an updated solar flux table is available for use with DAS 2.1. Please go to the Orbital Debris Website at https://www.orbitaldebris.jsc.nasa.gov/mitigation/debris-assessment-software.html to download the updated table and subscribe for email alerts of future updates.

UPCOMING MEETINGS

3-8 August 2019: 33rd Annual Small Satellite Conference, Logan, Utah, USA

Utah State University (USU) and the AIAA will sponsor the 33rd Annual AIAA/USU Conference on Small Satellites at the university's Logan campus, Utah, USA. With the theme of "Driving a Revolution," the 33rd conference will explore technical and development issues and the unique opportunities that arise from missions composed of tens, hundreds, or thousands of small satellites. Session topics include a review of the past 18 months of SmallSat activity, a preview of the next 18 months, ground systems, space access, educational programs, advanced technologies, and science/mission payloads. The abstract submission deadline passed on 1 February 2019. Additional information about the conference is available at https://smallsat.org/ .

17-20 September 2019: 20th Advanced Maui Optical and Space Surveillance Technologies Conference, Maui, Hawaii, USA

The technical program of the 20th Advanced Maui Optical and Space Surveillance Technologies Conference (AMOS) is anticipated to focus on subjects that are mission critical to Space Situational Awareness. The technical sessions include papers and posters on Adaptive Optics & Imaging; Astrodynamics; Machine Learning; Non-Resolved Object Characterization; Optical Systems & Instrumentation; Orbital Debris; Space Situational Awareness and Space-Based Assets. The abstract submission deadline passed on 1 March 2019. Additional information about the conference is available at https://amostech.com .

21-25 October 2019: 70th International Astronautical Congress (IAC), Washington, D.C., USA

The IAC will convene in Washington, D.C., USA in 2019 with a theme of "Space: the Power of the Past, the Promise of the Future." The IAA will organize the 17th Symposium on Space Debris as session A6 during the congress. Nine dedicated sessions are planned to cover all aspects of orbital debris activities, including measurements, modeling, hypervelocity impact, mitigation, remediation, and policy/legal/economic challenges for environment management. An additional joint session with the section B4.10 Small Satellites will be conducted to promote the long-term sustainability of space. Session A6 will also include an interactive presentation. The abstract submission deadline passed on 13 March 2019. Additional information for the 2019 IAC is available at https://www.iac2019.org/ .

9-12 December 2019: The First International Orbital Debris Conference (IOC), Sugar Land, Texas, USA

The first of this "once-every-4-years" conference series will be initiated 9-12 December 2019 in Sugar Land (greater Houston area), Texas, USA. The conference goal is to highlight orbital debris research activities in the United States and to foster collaborations with the international community. The 4-day conference will cover all aspects of micrometeoroid and orbital debris research, mission support, and other activities. Topics to be covered include radar, optical, in situ, and laboratory measurements; engineering, long-term environment, and reentry modeling; hypervelocity impacts and protection; and mitigation, remediation, policy, and environment management. The abstract submittal deadline passed on 29 April 2019. The conference announcement is available at https://www.hou.usra.edu/meetings/orbitaldebris2019/ .

14-16 January 2020: 2nd International Academy of Astronautics (IAA) Conference on Space Situational Awareness (ICSSA), Washington, D.C., USA

The International Academy of Astronautics (IAA), the American Institute of Aeronautics and Astronautics (AIAA), and the University of Florida's Mechanical and Aerospace Engineering Dept. will convene the 2nd IAA Conference on Space Situational Awareness in Washington, D.C., USA. Technical sessions include, but are not limited to, resident space object and Near Earth Object sensing, identification, forecasting, tracking, proximity operations, risk assessment, debris removal, drag assisted reentry, and deorbiting technologies. The abstract submission deadline is 15 August 2019. Additional information about the conference is available at http://reg.conferences.dce.ufl.edu/ICSSA/ .

SATELLITE BOX SCORE

(as of 30 June 2019, cataloged by the U.S. SPACE SURVEILLANCE NETWORK)

Country/ Organization	Spacecraft*	Rocket Bodies & Debris	Total
CHINA	356	3688	4044
CIS	1527	5062	6589
ESA	89	56	145
FRANCE	64	492	556
INDIA	97	157	254
JAPAN	175	115	290
USA	1778	4803	6581
OTHER	943	122	1065
TOTAL	5029	14495	19524

** active and defunct*

Visit the NASA Orbital Debris Program Office Website

www.orbitaldebris.jsc.nasa.gov

Technical Editor
Phillip Anz-Meador, Ph.D.

Managing Editor
Debi Shoots

Correspondence can be sent to:

J.D. Harrington
j.d.harrington@nasa.gov

or to:

Noah Michelsohn
noah.j.michelsohn@nasa.gov

National Aeronautics and Space Administration
Lyndon B. Johnson Space Center
2101 NASA Parkway
Houston, TX 77058

www.nasa.gov
https://orbitaldebris.jsc.nasa.gov/

INTERNATIONAL SPACE MISSIONS

01 April – 30 June 2019

Intl.* Designator	Spacecraft	Country/ Organization	Perigee Alt. (KM)	Apogee Alt. (KM)	Incli. (DEG)	Addnl. SC	Earth Orbital R/B	Other Cat. Debris
1998-067	ISS dispensed payloads	various	405	416	51.6	5	0	0
2019-018A	EMISAT	INDIA	733	760	99.7	28	1	0
2019-019A	PROGRESS MS-11	RUSSIA	408	418	51.6	0	1	0
2019-020A	O3B FM20	O3B	8063	8069	0.0	0	1	0
2019-020B	O3B FM19	O3B	8062	8070	0.0			
2019-020C	O3B FM17	O3B	8062	8070	0.0			
2019-020D	O3B FM18	O3B	8062	8070	0.0			
2019-021A	ARABSAT 6A	ARABSAT	35780	35796	0.0	0	1	0
2019-022A	CYGNUS NG-11	USA	408	418	51.6	0	1	0
2019-023A	BEIDOU 3 IGSO-1	CHINA	35715	35850	55.0	0	1	0
2019-024A	TIANHUI 2-01A	CHINA	514	517	97.5	0	1	4
2019-024C	TIANHUI 2-01B	CHINA	514	517	97.5			
2019-025A	DRAGON CRS-17	USA	396	417	51.6	0	0	2
2019-026A	AFOTEC-1	USA	499	511	40.0	0	2	0
2019-026B	SPARC-1	USA	493	511	40.0			
2019-026E	HARBINGER	USA	498	511	40.0			
2019-027A	BEIDOU 2 G8	CHINA	35773	35801	1.8	0	1	0
2019-028A	RISAT 2B	INDIA	550	558	37.0	0	1	0
2019-029A	OBJECT A	USA	546	552	53.0	59	0	4
2019-030A	COSMOS 2534 (GLONASS)	RUSSIA	19098	19162	64.8	0	1	0
2019-031A	YAMAL 601	RUSSIA	35778	35796	0.0	0	1	1
2019-032A	OBJECT A	CHINA	563	578	45.0	6	1	7
2019-033A	RCM-1	CANADA	584	605	97.8	0	0	0
2019-033B	RCM-3	CANADA	584	604	97.8			
2019-033C	RCM-2	CANADA	584	604	97.8			
2019-034A	AT&T T-16	USA	EN ROUTE TO GEO			0	1	1
2019-034B	EUTELSAT 7C	EUTELSAT	EN ROUTE TO GEO					
2019-035A	BEIDOU 3 IGSO-2	CHINA	EN ROUTE TO GEO			0	1	0
2019-036F	DSX	USA	5994	12012	42.2	17	1	0
2019-037A	OBJECT A	USA	451	461	45.0	6	2	1

** Intl. = International; SC = Spacecraft; Alt. = Altitude; Incl. = Inclination; Addnl. = Additional; R/B = Rocket Bodies; Cat. = Cataloged*